correction may be of the order of 1 Mev for very broad levels. It is therefore evident that the energy levels listed in the diagrams are only qualitatively related to the characteristic energies of the nuclei.

These sequences of low excited states of simple nuclei exhibit two striking features: (1) large spin-orbit splitting; (2) good correlation with an independent particle model. It appears that the single particle approximation is a good starting point for more exact study. To explain the large spin-orbit splitting, however, it may be necessary to consider specific nucleon-nucleon spin-orbit interactions.[9]

* Work supported by the AEC and the Wisconsin Alumni Research Foundation.

† AEC Predoctoral Fellow.

‡ Kimberly-Clark Fellow.

[1] M. G. Mayer, Phys. Rev. **78**, 16 (1950).

[2] E. Feenberg and K. C. Hammack, Phys. Rev. **75**, 1877 (1949).

[3] D. R. Inglis, Phys. Rev. **82**, 181 (1951); R. K. Adair, Phys. Rev. **82**, 750 (1951).

[4] Freier, Lampi, Sleator, and Williams, Phys. Rev. **75**, 1345 (1949); C. L. Critchfield and D. C. Dodder, Phys. Rev. **76**, 602 (1949); G. Goldhaber and R. M. Williamson, Phys. Rev. **82**, 495 (1951); Laubenstein, Laubenstein, Mobley, and Koester, Phys. Rev. **81**, 654(A) (1951); Bashkin, Petree, and Mooring, Phys. Rev. **82**, 378 (1951); H. L. Jackson and A. Galonsky, to be published.

[5] These analyses are feasible because the spin of the target nucleus is zero; hence, the total angular momentum J of a compound state is $L\pm\frac{1}{2}$, where L is the orbital angular momentum of the incident particle. The $\pm$ ambiguity is removed by conservation of parity, and the designation of a level by $S, P, D, \cdots$ is merely a statement of this fact, which does not imply that orbital angular momentum is conserved.

[6] Mooring, Goldberg, Kaufmann, Koester, and Saxon (to be published).

[7] E. P. Wigner and L. Eisenbud, Phys. Rev. **72**, 29 (1947); T. Teichmann, Ph.D. Dissertation, Princeton (1949).

[8] J. B. Ehrmann, Phys. Rev. **81**, 412 (1951).

[9] C. H. Blanchard and R. Avery, Phys. Rev. **81**, 35 (1951).

Proton-Proton Scattering Near 30 Mev*

FRANKLIN L. FILLMORE†
Radiation Laboratory, Department of Physics, University of California, Berkeley, California
(Received July 9, 1951)

THE work reported in an earlier paper[1] has been continued with a few improvements in technique. The entire apparatus was completely overhauled, and mechanical tolerances in the plate holder were carefully checked. The beam collimator was lengthened to a total of 21 inches, and the three graphite diaphragms shown in Fig. 7 of reference 1 were spaced so that the photographic plates were completely shielded from the $\frac{1}{16}$-inch and $\frac{3}{32}$-inch diaphragms. The lengthening of the collimator reduced the background of slit scattered tracks, making the observation of low angle tracks in the photographic emulsion more reliable. By using swaths which were less than one inch from the axis of the plate holder it was possible to observe tracks whose scattering angles ranged from 5° to 82° in the laboratory system. Plates from the same photographic emulsion batch were used as in the earlier work.

A set of three runs was made and results of these are reported below. Run 46 was the scattering run. Run 44 was a background run in which the scattering chamber was evacuated, while run 47 was a background run which was in all respects like a scattering run except that a molybdenum tube of $\frac{3}{4}$ inch diameter and 0.030-inch wall thickness was inserted axially in the scattering chamber so as to completely surround the beam and thus prevent scattered protons from reaching the plates. Tracks observed in the photographic plates for this run must be due to knock-on protons produced by neutrons in the hydrogen or in the material of the plate holder. The conditions prevailing during each run are summarized in Table I.

The criteria for reading tracks were the same as described in Sec. III-B of reference 1. Each swath was 2.300 inches long and 127±0.5 microns wide. The tracks were counted by Mr. R. C. Terzian, to whom the author is greatly indebted, and over half of the counts were checked by the author to determine the reliability of the counting. In order to speed the gathering of data in the region of small scattering angles, it was decided to try counting only tracks whose scattering angles were in the intervals 5° to 26° and 64° to 82° in the laboratory system. However, after twelve swaths had been counted in this manner, it was decided that the increase in speed was too small to justify the decrease in the reliability of counting tracks, so the method was abandoned. This accounts for the low number of tracks shown in Table I for the angular interval from 26° to 64°. All 1129 of the tracks counted in this manner were checked by the author, as were half of the swaths in which all of the tracks were counted. Since the number of tracks missed by Mr. Terzian amounted to only 1.5 percent, it was assumed in the cross section calculation that no tracks were missed on swaths which were counted by both observers. The number of tracks missed by Mr. Terzian on twelve swaths is given in column 3 of Table II. Column 4 is included to show that the two observers disagreed on only 0.56 percent of the tracks checked.

TABLE I. Summary of runs.

Run No.	Type of run	Time for pressure to reach 10^{-4} mm (sec)	Temp. (°C)	Pressure (mm of Hg)	Charge collected (coulombs ×10⁸)	Number of swaths scanned
44	background	0.6	···	10^{-4}	1.095	8
46	scattering	0.5	19.1	764.1	1.083	36
47	background	0.4	19.1	764.1	1.065	8

In order to enable the reader to visualize the types of all tracks on the plates a random swath $\frac{1}{2}$ inch long was scanned on each of the six plates of run 46. Of a total of 689 tracks of all kinds observed, 360 were judged to represent bona fide scattered protons, 320 were obviously no good, and 9 were spurious tracks which although appearing good failed to conform to all four of the criteria for good tracks.

As was shown in reference 1, the number of scattered protons should be symmetric about 45° in the laboratory system. Data in column 2 of Table II show that this is so, particularly at low scat-

TABLE II. Summary of data.

Angular interval (θ_{lab})	Total number of tracks counted	Number of tracks missed in 12 swaths by R.C.T.	Number of tracks on 12 swaths on which F.L.F. and R.C.T. disagreed	Number of tracks in both background runs
5° to 6°	60	2	0	2
6° to 10°	204	7	0	0
10° to 14°	246	4	2	0
14° to 18°	343	5	0	0
18° to 22°	463	5	0	0
22° to 26°	576	2	2	0
26° to 30°	436	2	1	1
30° to 34°	455	0	0	0
34° to 38°	527	2	0	0
38° to 42°	523	1	0	0
42° to 48°	761	0	0	0
48° to 52°	506	2	1	0
52° to 56°	483	1	1	0
56° to 60°	430	0	1	0
60° to 64°	398	0	1	0
64° to 68°	525	1	2	0
68° to 72°	464	0	4	0
72° to 76°	338	1	3	1
76° to 80°	267	2	0	3
80° to 82°	82	14	1	0
Total	8087	51	19	7

Of the 8087 tracks counted, 1129 were on swaths where tracks with scattering angles from 26° to 64° were omitted, 3432 of the remaining were checked by F.L.F., and 3526 were unchecked.

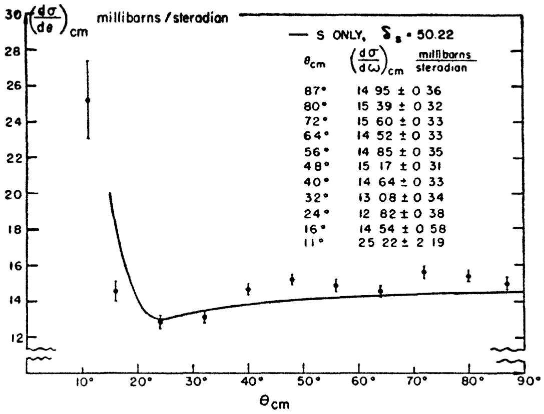

FIG. 1. Data based on 8087 tracks tabulated from run 46. The probable errors indicated on the graph are just those due to statistics. The *s*-wave curve shown was taken from Fig. 17 of reference 1 and is included here in order to facilitate the comparison of the present data with the earlier results.

tering angles. While the data near 45° do not show as good symmetry as one might hope, it is felt that the lack of symmetry is not serious and is accounted for statistically.

The primary energy was determined by the method described in reference 1. The range and scattering angle was measured for 202 tracks and a plot made from which the mean range at 45° was found to be 1120±4.3 microns. This corresponds to an energy of 30.14±0.08 Mev before scattering.

The cross sections were calculated by reflecting the raw data about 45° in the laboratory system and then applying Eq. (20) of reference 1 to each angular interval. This was done for each pair of swaths and the results averaged to give the uncorrected cross section. Corrections for background and number of tracks missed were then applied, giving the final results which are plotted in Fig. 1. The relative probable errors which are shown in Fig. 1 were obtained from the counting statistics. The probable error of the absolute cross section was found in the manner described in reference 1 to be 2.68 percent. The error due to lack of beam centering in the scattering chamber was found to be less than 0.2 percent. This correction was not applied to the cross section.

As can be seen from Fig. 1, these results do not conflict with the results reported earlier.[1,2] The high cross section at low angles which was not investigated in the earlier work is in qualitative agreement with expectations.

* This work was performed under the auspices of the AEC.
† Now with North American Aviation, Inc.

[1] Franklin L. Fillmore, Phys. Rev. **79**, 57 (1950).
[2] Franklin L. Fillmore, Phys. Rev. **79**, 71 (1950).

j-j Coupling Shell Model and Beta-Decay

H. HORIE AND M. UMEZAWA
Physics Department, University of Tokyo, Tokyo, Japan
(Received June 12, 1951)

BECAUSE of the success of the nuclear shell structure,[1] it seems probable that the individual particle model for nuclear structure has been given a rather strong foundation. However, Wigner's concept of supermultiplets[2] does not hold, since there is a strong spin-orbit interaction according to Mayer's shell model. On the other hand, we may assume charge independence of nuclear forces so far as the nuclear structure is concerned. Therefore, the charge multiplicity of nuclear states is still a good quantum number, especially for light nuclei.

We calculate the nuclear matrix elements for allowed β-transitions based on the above-mentioned assumptions. According to Fermi's β-decay theory,[3] the nuclear matrix elements related to the allowed transitions are $\int 1$ and $\int \boldsymbol{\sigma}$. These matrix elements, except for the radial parts (for the time being we shall not write them explicitly), are evaluated in the $TJT_\zeta M_J$-scheme, where T is the charge multiplicity, J the total angular momentum, T_ζ is the third component of T (i.e., half of neutron excess), and M_J is the z component of J. The calculations are similar to the atomic case in the SLM_SM_L-scheme.

In the j^n configurations, those matrix elements for the transitions $j^nTJT_\zeta \rightarrow j^nT'J'T_\zeta \pm 1$ are given as follows:

$$|\textstyle\int 1|^2 = |(TJT_\zeta \pm 1 M_J|\Sigma_i \tau_i^\pm|TJT_\zeta M_J)|^2 = (T \mp T_\zeta)(T \pm T_\zeta + 1),$$

$$\begin{aligned}|\textstyle\int \boldsymbol{\sigma}|^2 &= [3/(2J+1)]\Sigma M_J|(T'J'T_\zeta \pm 1 M_J|\Sigma_i \tau_i^\pm \sigma_{iz}|TJT_\zeta M_J)|^2\\ &= [2/(2J+1)](j\|\sigma\|j)^2(j^nT'J'\|V^{(11)}\|j^nTJ)^2 V(T'T1;\\ &\qquad -T_\zeta \pm 1 T_\zeta \pm 1)^2,\end{aligned}$$

where the notation of Racah[4] is used and the values of $(j\|\boldsymbol{\sigma}\|j')$ are given in the following formulas. When $n=1$ (one particle case), they become

$$|\textstyle\int 1|^2 = 1,$$

$$|\textstyle\int \boldsymbol{\sigma}|^2 = (1/2j+1)(j\|\sigma\|j)^2 = \begin{cases} (2l+3)/(2l+1) & (j=l+\frac{1}{2}) \\ (2l-1)/(2l+1) & (j=l-\frac{1}{2}) \end{cases}.$$

For, other configurations, we may evaluate the matrix elements by a trivial generalization. For example (for the one-particle casee, we have

$$|\textstyle\int \boldsymbol{\sigma}|^2 = (1/2j+1)(j'\|\sigma\|j)^2 = \begin{cases} 4l/(2l+1) & (j=l+\frac{1}{2} \rightarrow j'=l-\frac{1}{2}) \\ 4(l+1)/(2l+1) & (j=l-\frac{1}{2} \rightarrow j'=l+\frac{1}{2}) \end{cases}.$$

Of course, these results agree with those of Konopinski. We have calculated the matrix elements for more complicated configurations when they were necessary, but do not show them all here for the sake of simplicity.

The squares of total matrix elements $|M|^2$ for allowed β-transitions should be linear combinations of $|\int 1|^2$ and $|\int \boldsymbol{\sigma}|^2$ which are evaluated above. By the relation

$$ft|M|^2 = 2\pi^3 \log(2/G^2),$$

the experimental ft values multiplied by $|M|^2$ should be constant for all allowed β-transitions, though there are still ambiguities of $|M|^2$ caused by radial overlapping. For β-transitions of mirror nuclei, we examined this situation, taking $|M|^2$ as $|\int 1|^2$ and $|\int \boldsymbol{\sigma}|^2$ separately. The results are shown in Table I. We see at once the values of $ft|\int \boldsymbol{\sigma}|^2$ vary too violently even if the variation of radial overlapping is taken into account. On the contrary, $ft|\int 1|^2$ show fairly constant values. Therefore, it seems reasonable to consider that the Fermi-type interaction is the main part of the allowed β-transitions and that the Gamow-Teller one is subsidiary.

For most of the allowed β-transitions of even nuclei and odd nuclei other than mirror nuclei, only the matrix element $\int \boldsymbol{\sigma}$ is

TABLE I. β-decay of mirror nuclei.[a]

	Configuration	$ft\lvert\int 1\rvert^2/10^3 = ft/10^3$	$\lvert\int \boldsymbol{\sigma}\rvert^2$	$ft\lvert\int \boldsymbol{\sigma}\rvert^2/10^3$
$n \rightarrow H^1$	$(s_{1/2})^1$	1–3	3	3–9
$H^3 \rightarrow He^3$	$(s_{1/2})^{-1}$	1.1	3	3.3
$C^{11} \rightarrow B^{11}$	$(p_{3/2})^{-1}$	3.9	5/3	6.5
$N^{13} \rightarrow C^{13}$	$(p_{1/2})^1$	4.8	1/3	1.6
$O^{15} \rightarrow N^{15}$	$(p_{1/2})^{-1}$	3.7	1/3	1.2
$F^{17} \rightarrow O^{17}$	$(d_{5/2})^1$	2.2[b]	7/5	3.1
$Ne^{19} \rightarrow F^{19}$	$(s_{1/2})^{-1}$	2.0	3	6.1
$Si^{27} \rightarrow Al^{27}$	$(d_{5/2})^{-1}$	3.6	7/5	5.0
$P^{29} \rightarrow Si^{29}$	$(s_{1/2})^1$	3.8	3	11.4
$S^{31} \rightarrow P^{31}$	$(s_{1/2})^{-1}$	3.4	3	10.2
$Cl^{33} \rightarrow S^{33}$	$(d_{3/2})^1$	4.0	3/5	2.4
$A^{35} \rightarrow Cl^{35}$	$(d_{3/2})^3$	3.4	121/375	1.1
$Sc^{41} \rightarrow Ca^{41}$	$(f_{7/2})^1$	2.6	9/7	3.3

[a] The ft-values used are calculated by making use of G. L. Trigg and E. Feenberg's curves (see reference 5).
[b] The maximum energy of F^{17} decay is taken from Natl. Bur. Standards (U. S.) Circ. 499 (1950).